



Describing the Wavefront Aberrations of the Hexagonal Aperture Using Modified Zernike Polynomials

Loay K. Abood¹, Shatha M. Al-Hilly², Raaid Nawffee Hassan^{*3}

¹Department of Computer Science, College of Science, University of Baghdad, Baghdad, Iraq

²Department of Physics, College of Science, University of Baghdad, Baghdad, Iraq

³Department of Astronomy, College of Science, University of Baghdad, Baghdad, Iraq

*raadnoffi742000@yahoo.com

Abstract

The concept of the optical telescope is the primary mirror design, the Next Generation Segmented Optical Telescope (NGST) with hexagonal segment of spherical primary mirror can provide a 3 arc minutes field of view. Extremely Large Telescopes (ELT) in the 100m dimension would have such unprecedented scientific effectiveness that their construction would constitute a milestone comparable to that of the invention of the telescope itself and provide a truly revolutionary insight into the universe. The scientific case and the conceptual feasibility of giant filled aperture telescopes was our interested. Investigating the requirements of these imply for possible technical options in the case of a 100m telescope. For this telescope the considerable interest is the correction of the optical aberrations for the coming wavefront, the modified Zernike polynomials for hexagonal aperture were used to describe the wavefront aberrations and to predict the initial state for the adaptive optics corrections.

Keyword: Zernike polynomials, Wavefront aberration, Very large telescope, PSF, MTF

وصف جبهة الموجة المشوهة لفتحة سداسية باستخدام متعددة حدود زرنايك

لؤي كاظم عبود¹, شذى محمد الحلي², رائد نوفي حسان^{*3}

¹قسم الحاسبات, كلية العلوم, جامعة بغداد, بغداد, العراق

²قسم الفيزياء, كلية العلوم, جامعة بغداد, بغداد, العراق

³قسم الفلك والفضاء, كلية العلوم, جامعة بغداد, بغداد, العراق

الخلاصة

مفهوم التلسكوب البصري هو في تصميم المرآة الأولية، الجيل القادم من التلسكوبات البصرية المجزأة بقطع سداسية للمرآة الكروية الأولية يمكن ان يوفر مجال رؤيا بمقدار 3 دقائق قوسية . التلسكوبات الكبيرة جداً بابعاد 100 م يملك هكذا تاثيرات علمية لا سابق لها بتركيبها ستشكل معلماً يمكن مقارنته باكتشاف التلسكوب نفسه ويوفر ثورة حقيقية لتفهمنا وتبصرنا للكون. الحالة العلمية والتصور المعقول للفتحات العملاقة للتلسكوبات هي موضع اهتمامنا. تحقيق المتطلبات لهذا تلسكوب يتضمن خيارات التقنية الممكنة في حالة 100م تلسكوب. الاهتمام الكبير لهذا النوع من التلسكوب هو في تصحيح التشوهات البصرية لجبهة الموجة القادمة، استخدمت متعددة حدود Zernike المطورة للفتحة السداسية لوصف تشوهات جبهة الموجة وتخمين الحالة الاساسية لتصحيحات البصريات المطورة.

Introduction

To determine and apply the proper correction that will eliminate or minimize different types of aberrations, their characteristics must be first captured and quantitatively described. The wave aberration function suits this purpose well because it completely describes a cumulative effect of the optical system on light passing through every location in the aperture [1].

For the NGST can be used the modified Zernike polynomials for hexagonal aperture to form a complete set of functions or modes. This makes them suitable for accurately describing wave aberrations as well as for data fitting. They are usually expressed in polar coordinates, and are readily convertible to Cartesian coordinates. These polynomials are mutually orthogonal, and are therefore mathematically independent, making the variance of the sum of modes equal to the sum of the variances of each individual mode. They can be scaled so that non-zero order modes have zero mean and unit variance [1, 2]. This puts all modes in a common reference frame that enables meaningful relative comparison between them.

Describing The Wave Aberration Function using Zernike Polynomials

The wave aberration function is expressed as a weighted sum of Zernike polynomials (Z_n^m) [2] [3]:

$$W(\rho, \theta) = \sum_n^k \sum_{m=-n}^n W_n^m Z_n^m(\rho, \theta)$$

$$W(\rho, \theta) = \sum_n^k \left\{ \begin{array}{l} \sum_{m=-n}^{-1} W_n^m (-N_n^{|m|}(\rho) \sin(m\theta)) + \\ \sum_{m=0}^n W_n^m (N_n^m R_n^{|m|}(\rho) \cos(m\theta)) \end{array} \right\} \dots(1)$$

Where

k is the polynomial order of the expansion.

W_n^m is the coefficient of the Z_n^m mode in the expansion.

W_n^m is equal to the rms wavefront error for that mode.

For computational purposes it may be more convenient to express the wave aberration in rectangular coordinates and use the single indexing scheme:

$$W(x, y) = \sum_{j=0}^{j_{max}} W_j Z_j(x, y) \dots\dots(2)$$

where

$$W_j = W_n^m \text{ and } Z_j(x, y) = Z_n^m(x, y)$$

$$j = \frac{n(n+2)+m}{2}$$

j_{max} refers to the highest mode number included in the expansion.

n order of the radial polynomial.

m azimuthal or angular frequency.

(ρ, θ) polar coordinates where $0 \leq \rho \leq 1$ and

$0 \leq \theta \leq 2\pi$.

Orthonormal Polynomial for Hexagonal Apertures

It is quite common in optical design and testing using Zernike circle polynomials to describe the aberration of a system. These polynomials have the advantage that they represent balanced aberrations. Because of their orthogonality across a circular aperture, the Zernike expansion coefficients are independent of each other, each coefficient represents the standard deviation of the corresponding Zernike term (with exception of the piston term), and the variance of the aberration is equal to the sum of the coefficients. However, in the case of a large segmented mirror, the segments are typically hexagonal in the shape, as in the Keck telescope [4]. The advantage of the orthogonality of the polynomial can be lost because Zernike polynomials are not orthogonal over hexagonal region. Here, orthonormal polynomial for hexagonal apertures can be determined by the Gram-Schmidt orthogonalization of Zernike circle polynomial. The polynomial thus obtained can be depending on the sequence of the Zernike polynomials used in the orthogonalization process [5].

Figure 1 shows a unit hexagon inscribed inside a unit circle. Each side of the hexagon has a length of unity. The area of the hexagon is $A=3\sqrt{3}/2$. In Cartesian coordinates (x,y) , the aberration function for a hexagonal pupil or aperture can be expanded in terms of polynomials $H_j(x,y)$ that are orthonormal over the aperture [6]:

$$W(x, y) = \sum_j a_j H_j(x, y) \dots\dots\dots(3)$$

Where a_j is an expansion or the aberration coefficient of the polynomial $H_j(x,y)$. The

orthonormality of the polynomial is represented by:

$$\frac{2}{3\sqrt{3}} \int H_j H_j dx dy = \delta_{jj} \dots\dots\dots(4)$$

Where δ_{jj} stands for the Kronecker symbol, which equal to 1 only if when $j=j'$.

The hexagonal region of integration consists of five parts: rectangle ACDF, triangles AGB, GCB, DHE, and HFE with limits of integration $(-1/2, 1/2; -\sqrt{3}/2, \sqrt{3}/2)$, $(1/2, 1; \sqrt{3}(1-x), 0)$, $(1/2, 1; -\sqrt{3}(1-x), 0)$, $(-1, -1/2; 0, \sqrt{3}(1+x))$, and $(-1, -1/2; 0, \sqrt{3}(1+x))$, respectively.

The area of the unit hexagon is approximately 17.3% smaller than the area of the unit circle.

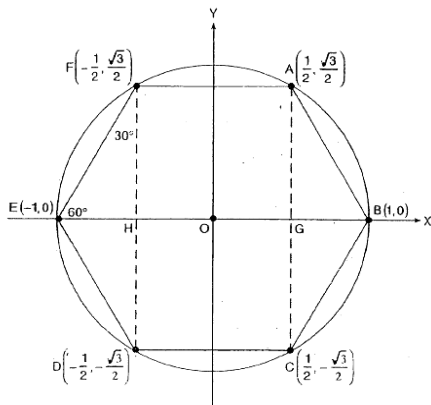


Figure1- Unit hexagon inscribed inside a unit circle showing the coordinates of its corners. Each side of the hexagon has a length of unity. The x axis passes through the corners B and E of the hexagon, and the y axis bisects its parallel sides AC and FD [5].

The relative value of the coefficients of the circle polynomials whose linear combination yields an orthonormal hexagonal polynomial H_k and the variance are given by:

$$a_j = -\frac{2}{3\sqrt{3}} \int W(x, y) H_j dx dy \dots\dots\dots(5)$$

$$\sigma^2 = \sum_j a_j^2 \quad j \neq 1 \dots\dots\dots(6)$$

Respectively, the mean value of each polynomial, except for $j=1$, is zero. The number of polynomial, i.e, the maximum value of j is increased until the variance is equal to the actual variance within a prechosen tolerance.

The orthonormal polynomials $H_j(x,y)$ can be obtained from the Zernike polynomials $Z_j(x,y)$ by Gram-Schmidt orthogonalization process [6]. Using abbreviated notation, where the argument (x,y) of the polynomial is omitted,

$$G_1 = Z_1 = 1$$

$$G_{j+1} = \sum_{k=1}^j c_{j+1,k} H_k + Z_{j+1}$$

$$H_{j+1} = \frac{G_{j+1}}{\|G_{j+1}\|} = \frac{G_{j+1}}{\left[\frac{1}{2} \int_{hexagon} G_{j+1}^2 dx dy \right]^{1/2}} \dots\dots\dots(7)$$

where

$$c_{j+1,k} = -\frac{2}{3\sqrt{3}} \int_{hexagon} Z_{j+1} H_k dx dy$$

Thus, the H -polynomial are obtained recursively starting with $H_1 = 1$. Each G and, therefore, H -polynomial is a linear combination of Zernike polynomials. The orthonormal H -polynomials represent the unit vectors of the space that spans the aberration function.

The Zernike circle polynomials are orthonormal over a circular pupil of unit radius is:

$$\int Z_j(x, y) Z_j(x, y) dx dy / \int dx dy = \delta_{jj} \dots\dots(8)$$

Substituting for the Zernike polynomial and noting that of an odd function over the hexagon is zero owing to its symmetry, it is possible to obtain:

$$G_2 = c_{21} H_1 + Z_2 = c_{21} Z_1 + Z_2 = Z_2 = 2x$$

$$H_2 = \frac{2x}{\left[\frac{1}{A} \int_{hexagon} 4x^2 dx dy \right]^{1/2}} = \sqrt{6/5} (2x) = 1.09545 Z_2$$

$$= 2\sqrt{6/5} \rho \sin \theta$$

where $A = -2/3 \sqrt{3}$

Similarly

$$H_3 = \sqrt{6/5} (2y) = 1.09545 Z_3 = 2\sqrt{6/5} \rho \cos \theta$$

$$c_{41} = 1/\sqrt{3}, \quad c_{42} = 0 = c_{43}$$

$$G_4 = (1/\sqrt{3}) Z_1 + Z_4 = \sqrt{3} (2\rho^2 - 5/6)$$

$$H_4 = \frac{\sqrt{3} (2\rho^2 - 5/6)}{\left[\frac{1}{A} \int_{hexagon} 3(2\rho^2 - 5/6)^2 dx dy \right]^{1/2}}$$

$$= \frac{\sqrt{3} (2\rho^2 - 5/6)}{\sqrt{43/60}}$$

$$= \sqrt{5/43} Z_1 + 2\sqrt{15/43} Z_4$$

$$= 0.34100 Z_1 + 1.18125 Z_4$$

$$= 2\sqrt{15/7} \rho^2 \sin 2\theta$$

The other polynomial can be obtained in similar manner as shown as in table (1).

Table 1 Orthonormal Hexagonal Polynomials in Polar Coordinates

H1 = 1
 H2 = 2 √(6/5) ρ sinθ
 H3 = 2 √(6/5) ρ cosθ
 H4 = 2 √(15/7) ρ² sin2θ
 H5 = √(5/43) (-5 + 12 ρ²)
 H6 = 2 √(15/7) ρ² cos2θ
 H7 = (4√(10)/3) ρ³ sin3θ
 H8 = 4 √(42/3685) (-14 ρ + 25 ρ³) sinθ
 H9 = 4 √(42/3685) (-14 ρ + 25 ρ³) cosθ
 H10 = 4 √(70/103) ρ³ cos3θ
 H11 = (10/3) √(7/99258181) (-10 (297 - 598 ρ²) ρ² sin2θ + 5413 ρ³ sin4θ)
 H12 = (30 / √(492583)) (-249 ρ²+ 392 ρ⁴) sin2θ
 H13 = (3 / √(1072205)) (737 - 5140 ρ²+ 6020 ρ⁴) cos2θ
 H14 = (30 / √(492583)) (-249 ρ²+ 392 ρ⁴) cos2θ
 H15 = (10/3) √(7/99258181) (10 (297 - 598 ρ²) ρ² cos2θ + 5413 ρ⁴ cos4θ)
 H16 = (2.17600248 ρ - 13.23551876 ρ³+ 16.15533716 ρ⁵) sinθ + 5.95928883 ρ⁵ sin5θ
 H17 = 4 √(5/97)(-22 ρ³+ 35 ρ⁵) sin3θ
 H18 = 2 √(6/1089382547) (70369 ρ- 322280 ρ³+ 309540 ρ⁵) sinθ
 H19 = 2 √(6/1089382547) (70369 ρ- 322280 ρ³+ 309540 ρ⁵) cosθ
 H20 = 4 √(385/295894589) (-3322 ρ³+4635 ρ⁵) cos 3θ
 H21 = (-2.17600248 ρ +13.23551876 ρ³ - 16.15533716 ρ⁵) cos θ + 5.95928883 ρ⁵ cos5θ

Calculating the Point Spread Function (PSF)

Aberrations negatively impact image quality. They change the size and shape of impulse response or point spread function (PSF), which blurs the image. In terms of frequency analysis, the frequency response of the optical system is reduced by phase distortion within the passband. The effects of aberrations can therefore be characterized by calculating the PSF of the optical system [8], [9]. The image of a point object formed by the optical system is the point spread function or impulse response. It is defined as [10], [11]:

$$PSF(x, y) = \frac{1}{\lambda^2 d^2 A_p} \left\| FT \left\{ p(x, y) e^{-i \frac{2\pi}{\lambda} W(x, y)} \right\} \right\|_{f_x = \frac{x}{\lambda d}, f_y = \frac{y}{\lambda d}}^2 \dots(9)$$

FT is the fourier Transform operator.
 d is the distance from the exit pupil to the image.

A_p is the area of the exit pupil.
 $P(x,y)$ define shape, size, and transmission of exit pupil.

$e^{-i \frac{2\pi}{\lambda} W(x, y)}$ Accounts for the phase deviations of the wavefront from a reference sphere.
 $W(x,y)$ is the wave aberration function at the exit pupil.

$P(x, y) = p(x, y) e^{-i \frac{2\pi}{\lambda} W(x, y)}$ is the generalized exit pupil function.

For visual applications it is often more convenient to express the PSF in terms of visual angle. These expressions are given by [12]:

$$PSF(\sin(\theta_x), \sin(\theta_y)) = \frac{\lambda^2}{A_p} \left\| FT \left\{ p(x, y) e^{-i \frac{2\pi}{\lambda} W(x, y)} \right\} \right\|^2$$

for small angle:

$$PSF(\theta_x, \theta_y) \cong \frac{\lambda^2}{A_p} \left\| FT \left\{ p(x, y) e^{-i \frac{2\pi}{\lambda} W(x, y)} \right\} \right\|^2 \dots\dots\dots(10)$$

Where:

$\frac{A_p}{\lambda^2}$ is the area of the exit pupil in unit of (wavelength)²

$p(x, y)$ defines shape, size (in unit of wave lengths), and transmission of exit pupil.

The calculations and computational domains are illustrated in Figure 2.

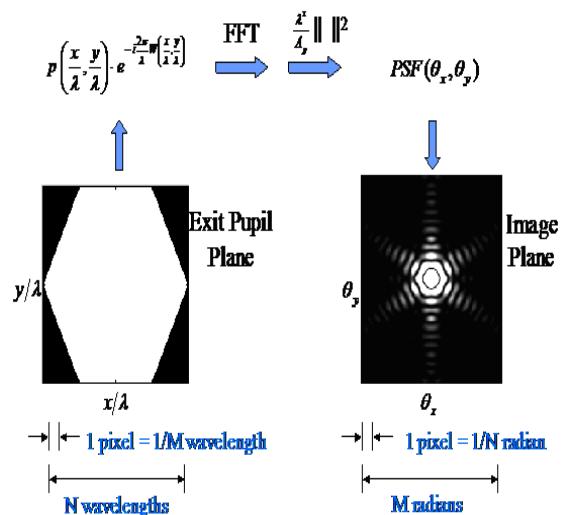


Figure 2-SPFPSFCalculationandComputational Domains

Utilize equation (10) to generate and plot the PSF for any wave aberration mode associated with any modified Zernike polynomial for hexagonal specification by (n, m):

(1,-1) y tilt, (1,1) x tilt, (2,-2), (2,2) astigmatism, (2,0) defocus, (3,-1), (3,1) coma, (3,-3), (3,3) trefoil, (4,0) spherical aberration and secondary coma, the diameter of the aperture is 100 pixel (equivalent to 100 μm), Root Mean Square (RMS)

wavefront error (in μm), and wavelength (in μm) are shown in Figures 3,7.

• **Double-Index Modified Zernike Polynomials (H)**

Figure 3 illustrated modified Zernike polynomials for hexagonal up to 5th order in a pyramid arrangement.

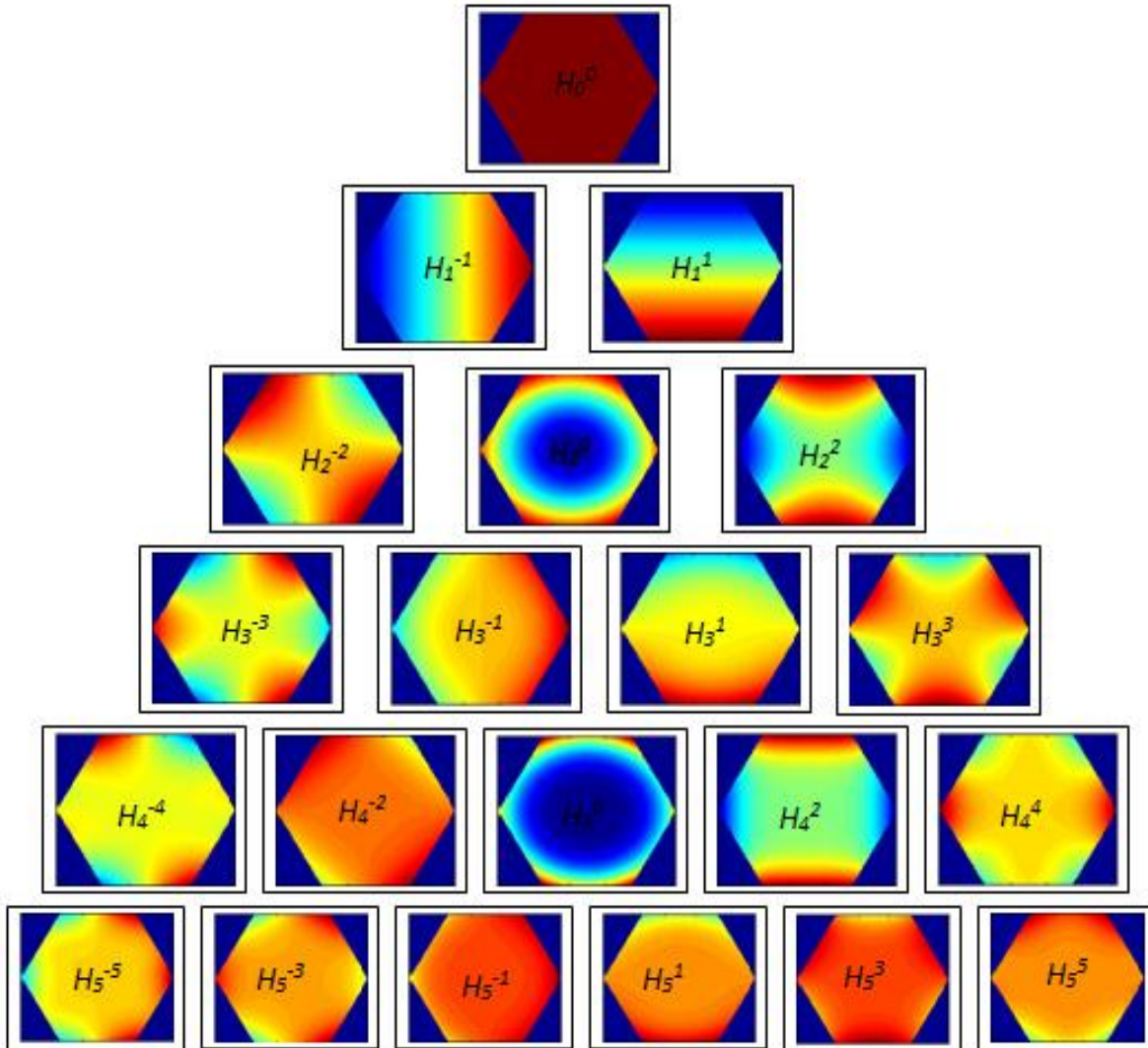


Figure 3- Modified Zernike polynomials up to 5th order

•Double-Index Modified Zernike Polynomial (H) PSFs

The image in Figure 4 shows the image of a point object (binary star) in the presence of polynomial aberration (image convolution with polynomials). The PSF images in Figure 5

illustrated their visual appearance, and to more explanation and representation of PSF cross-section in terms of visual angle (θ_x and θ_y) measured in mrad are shown in Figures 6,7.

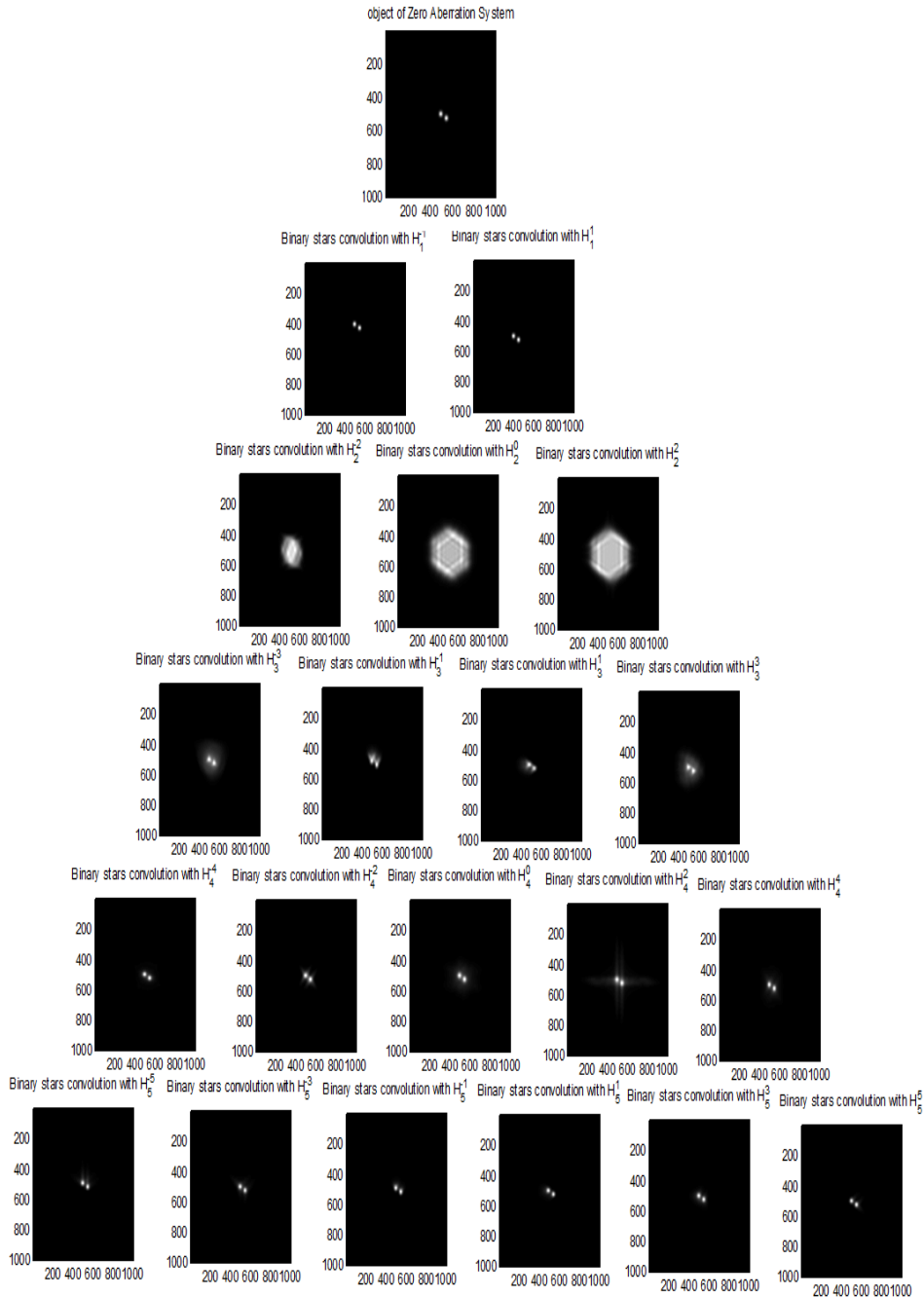


Figure 4-Image Convolution with Polynomials Aberration

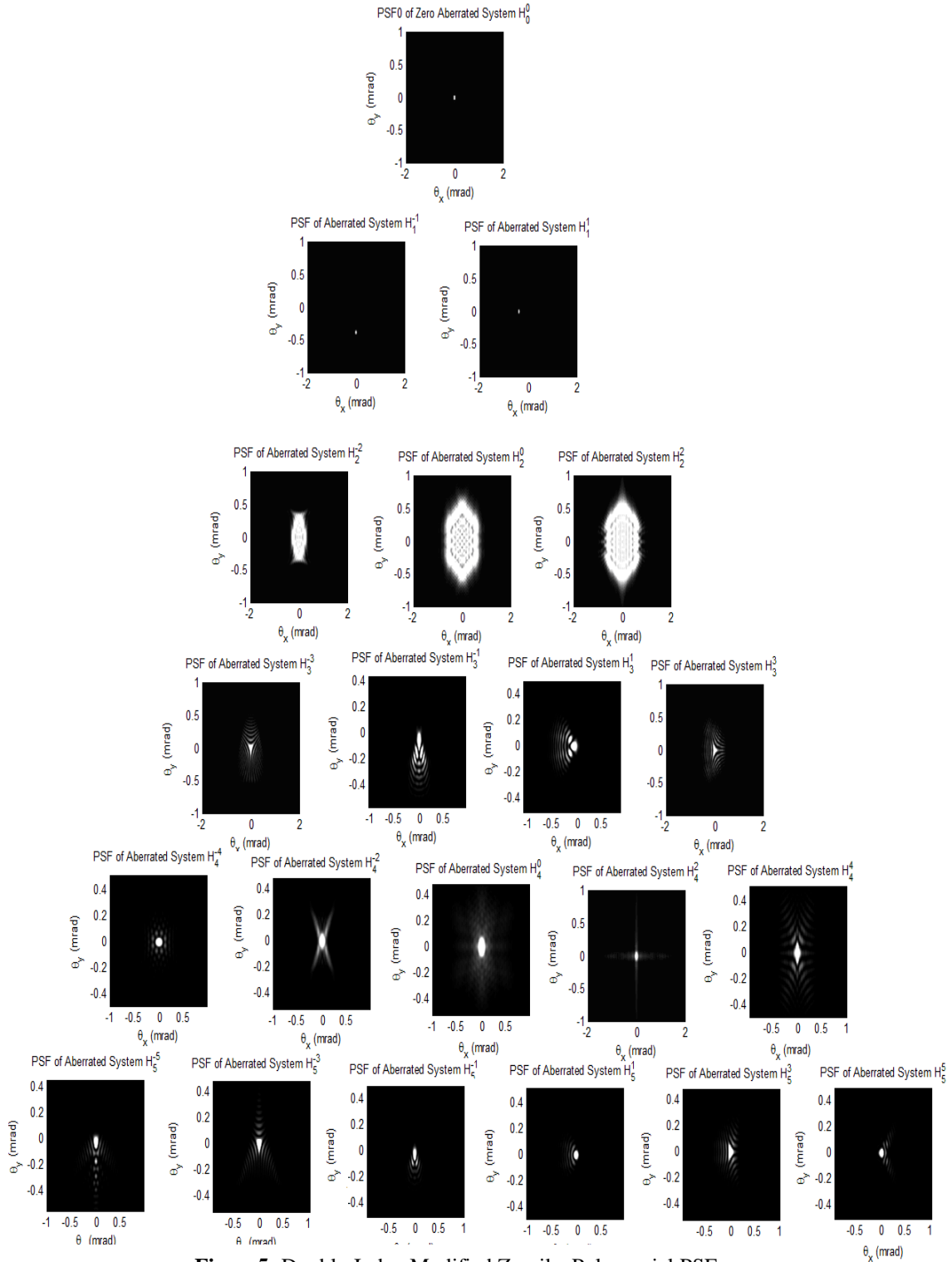


Figure5- Double-Index Modified Zernike Polynomial PSFs

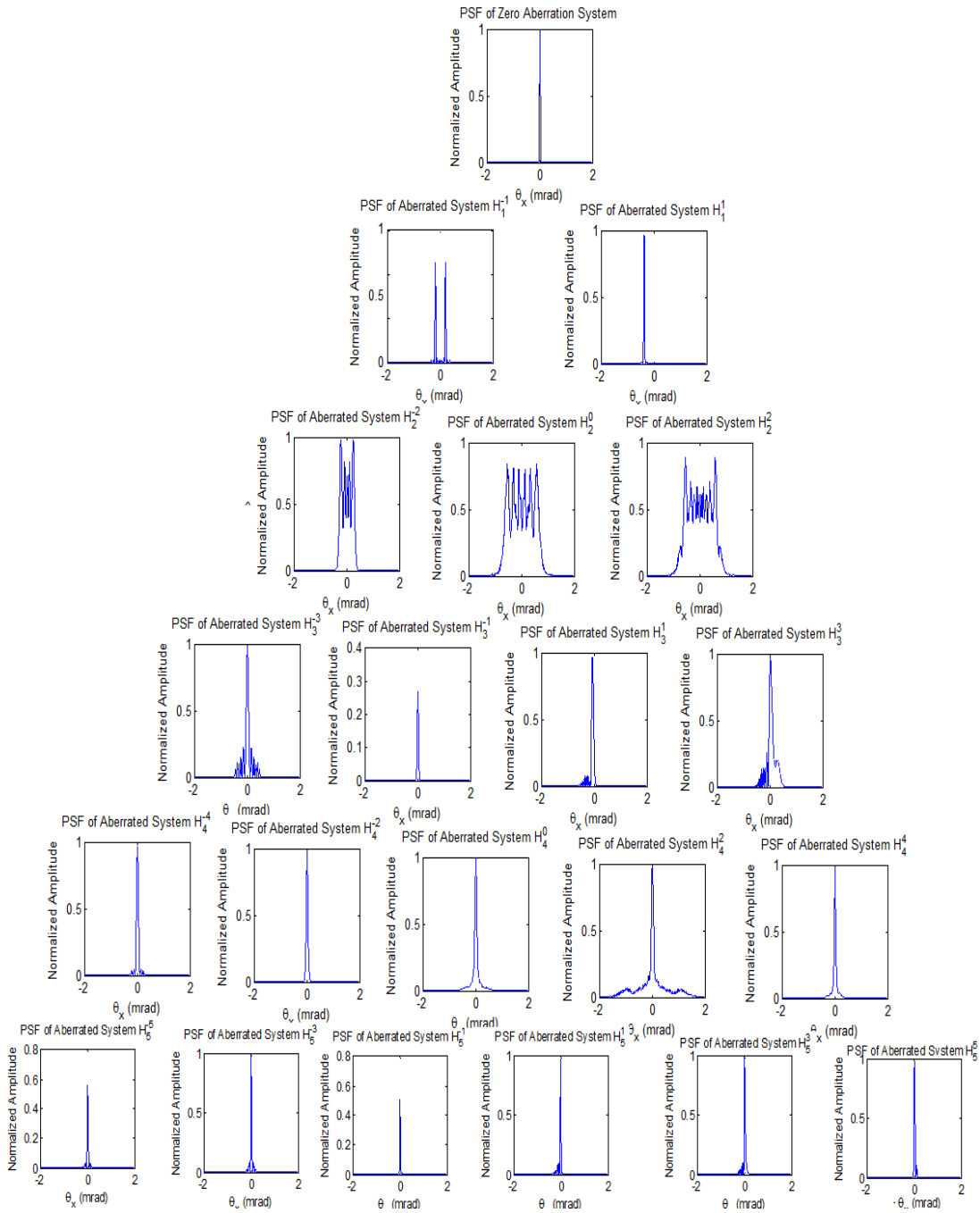


Figure 6- PSF Cross-Sections in Terms of Visual Angle θ_x (mrad)

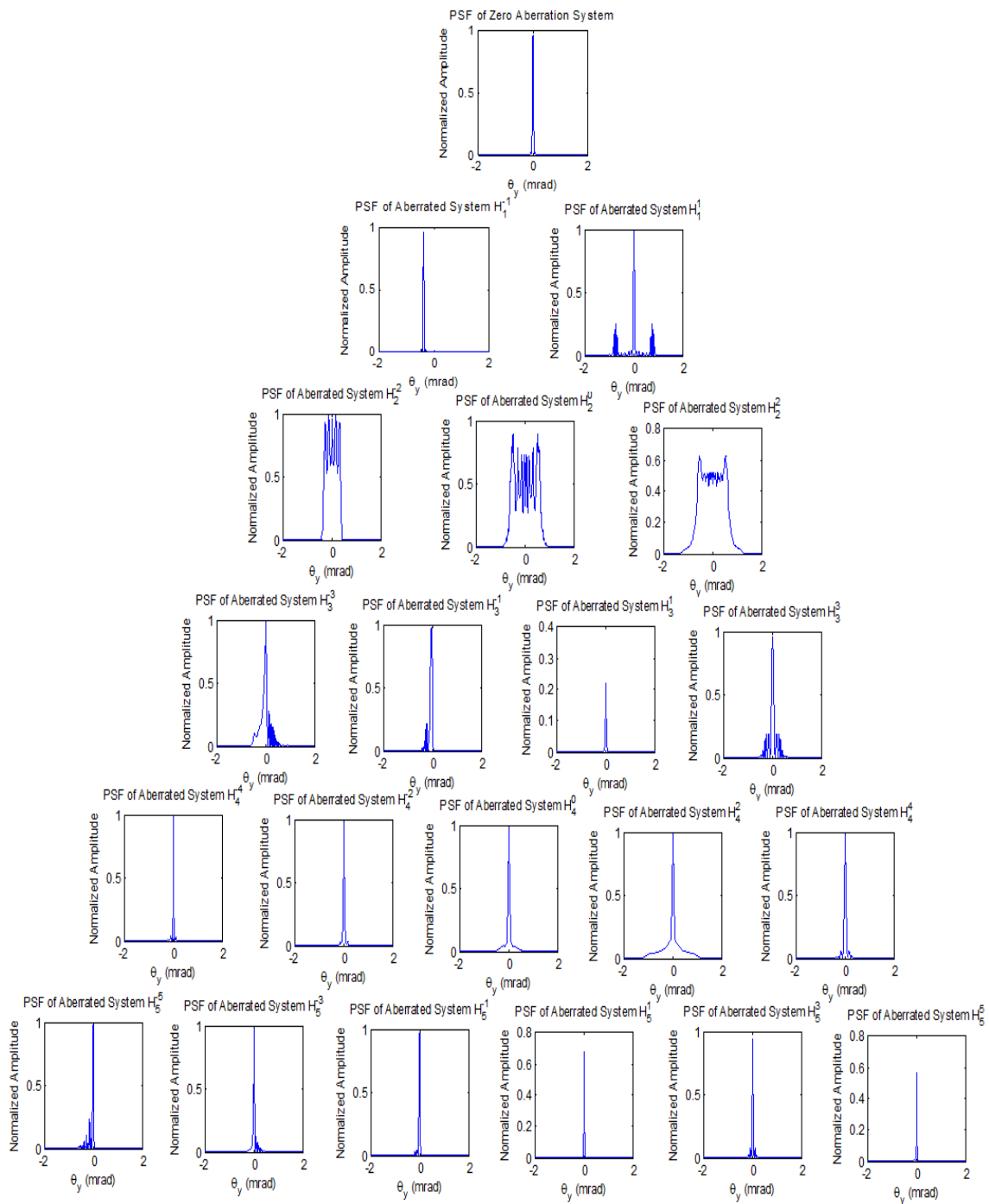


Figure 7- PSF Cross-Sections in Terms of Visual Angle θ_y (mrad)

Figure 8 shows the observed image as a result of almost types of aberration up to 5th order. The isometric plot in

Figure 9 illustrates its shape as produced in a deformable mirror in adaptive optics to correct and reduce aberrations from the incident at hexagonal aperture of the telescope

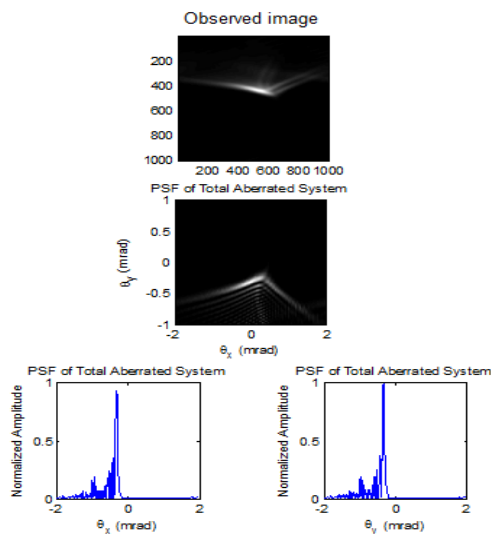


Figure 8- Shows the Result of the Accumulative H Modes (Observed Image)

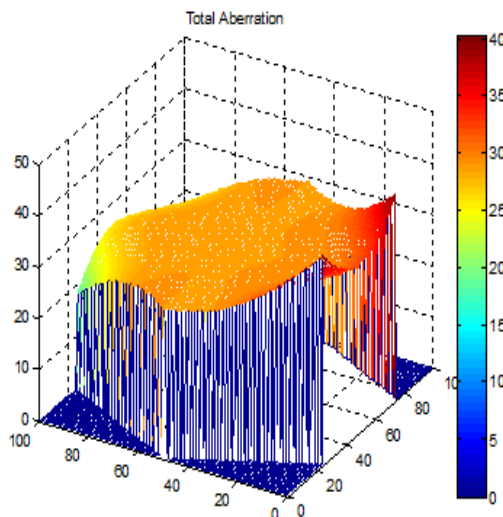


Figure 9- Isometric Plot Shows the Shape reduced in a Deformable Mirror in Adaptive Optics

Conclusions

Orthogonal polynomials have been considered for analysis of wavefronts across noncircular pupil such as hexagonal segments of a large mirror telescopes. From previous Figures 4,8 it can be noticed that this configuration is more sensitive to Seidel aberration except coma which is slightly less sensitive. The isometric plot Figure 9 can represent the initial state for adaptive optics correction.

References

1. Dunkl C. F., **1987**, *Orthogonal Polynomials on the Hexagon*, SIAM Journal on Applied Mathematics, Vol. **47**, no. 2, pp. 343-35
2. Thibos L. N., **1999**, *Handbook of Visual Optics*, Indiana University v. 4/99.
3. Mahajan V. N., **1995**, *Zernike polynomials and aberration balancing*, Appl. Opt., pp. 8057–8059, Proc. of SPIE Vol. 5173.
4. Chanan G., Troy M., Dekens F., Michaels S., Nelson J. and Mast T., **1998** *Phasing the Mirror Segments of the Keck Telescopes: the Broadband Phasing Algorithm*, Applied Optics, Vol. 37, no. 1.
5. Mahajan V. N. and Dai G.-m., **2008** *Orthonormal Polynomials for Hexagonal pupils: addendum*, J. Opt. Soc. / Vol. 33, no. 10.
6. Mahajan V. N. and Dai G.-m., **2007** *Orthonormal Polynomials in Wavefront Analysis: Analytical solution*, 2994 J. Opt. Soc. Am. A/Vol. 24, no. 9/September.
7. Dai G., **2007** „Systems and Methods for Wavefront Reconstruction for Aperture with Arbitrary shape”, Patent application number: 20100238407, Assignees: AMO Manufacturing USA, LLC World Intellectual Property Organization.
8. Tahir H. j., Parry N. R. A., Pallikaris A. and Murray I. J., **2009**, *Higher-order aberrations produce orientation-specific notches in the defocused contrast sensitivity function* Journal of Vision, vol. **9** no. 7 article 11.
9. Murray I. J., Elliott S. L., Pallikaris A., Werner J. S., Choi S. and Tahir H. J., **2010**, *The oblique effect has an optical component: Orientation-specific contrast thresholds after correction of high-order aberrations*, Journal of Vision, Vol. **10**, no. 11, article 10.
10. Goodman J. W., **1968**, *Introduction to Fourier Optics*, second edition, San Francisco: McGraw Hill.
11. Gaskill J. D., **1978**, *Linear Systems, Fourier Transforms, Optics*, New York: Wiley.
12. Bracewell R. N., **2000**, *The Fourier Transform and Its Applications*, McGraw Hill.